(c)2001 American Institute of Aeronautics & Astronautics or Published with Permission of Author(s) and/or Author(s)' Sponsoring Organization.

A01-16146

AIAA-2001-0232
Flow Quality Surveys of the NASA Glenn Icing Research Tunnel (2000 Tests)

Jose C. Gonsalez, E. Allen Arrington, and
Monroe R. Curry III
Dynacs Engineering Company, Inc.
Brook Park, OH

39th AIAA Aerospace Sciences Meeting & Exhibit
January 8–11, 2001 / Reno, NV

For permission to copy or republish, contact the American Institute of Aeronautics and Astronautics 1801 Alexander Bell Drive, Suite 500, Reston, VA 20191–4344

(c)2001 American Institute of Aeronautics & Astronautics or Published with Permission of Author(s) and/or Author(s)' Sponsoring Organization.

AIAA–2001–0232

FLOW QUALITY SURVEYS OF THE NASA GLENN ICING RESEARCH TUNNEL (2000 TESTS)

Jose C. Gonsalez,* E. Allen Arrington,† and Monroe R. Curry III‡
Dynacs Engineering Company, Inc.
Brook Park, Ohio 44142

Abstract

Major modifications were made to the NASA Glenn Icing Research Tunnel to improve both the icing and aero-thermal characteristics of the facility. The modifications included replacing the original folded heat exchanger with a flat heat exchanger, expanding the width of the tunnel loop to accept the larger flat heat exchanger, new corner turning vanes up and downstream of the heat exchanger and exit guide vanes downstream of the drive fan. Surveys using traversing probes were conducted at two stations in the tunnel to measure the effectiveness of the modifications on the local flow quality. When these data were compared with survey data collected in 1995, the results indicated significant improvement at both stations in terms of flow uniformity and decreased turbulence and flow angularity.

Symbols

a	Speed of sound, ft/sec
a,b,c,d	Hot wire calibration curve fit coefficients
E	Hot wire anemometer bridge voltage, volts
N	Number of data points
M	Mach number
P	Pressure, psi
R	Specific gas constant for air, 1716 $ft^2/(sec^2\ °R)$
T	Temperature, °F (display) or °R (calculations)
TI	Turbulence intensity, %
u	Hot wire axial velocity component, ft/sec
V	Velocity, ft/sec or mph
v	Hot wire transverse velocity component, ft/sec
α	Pitch flow angle, degrees
β	Yaw flow angle, degrees
γ	Ratio of specific heats, 1.4
σ	Standard deviation
θ	Hot wire sensor inclination angle, degrees

Subscripts

avg	Average or mean
c	Corrected
cal	Pertaining to probe calibration
eff	Effective hot wire velocity
HW	Pertaining to a hot wire probe
i	Hot wire sensor index, 1 or 2
j	Hot wire data point index
jet	Pertaining to the hot wire calibration jet
sensor	Pertaining to individual hot wire sensors
S	Static conditions
test	Pertaining to test conditions
T	Total or stagnation conditions
wa	Pertaining to a wind anemometer

Introduction

As part of the continuing efforts to upgrade and improve the test facilities at NASA Glenn, several major modifications were made to the Icing Research Tunnel (IRT). These modifications were aimed at improving the icing and aero-thermal characteristics of the IRT, as well as the operational efficiency of the facility. As this was a very extensive upgrade to the IRT and affected several key components of the tunnel, a comprehensive implementation and recommissioning plan was developed and executed to insure success.

The most significant modification was the replacement of the tunnel heat exchanger. The original heat exchanger was a folded or W-shaped configuration that provided maximum cooling area. An elevation view of the original folded heat exchanger is shown in Figure 1. While very effective in setting the low temperatures needed for icing conditions, the folded design had a negative impact on the aerodynamic flow quality. This, coupled with the fact that the aging heat exchange was becoming increasingly difficult to maintain, lead to the decision to replace the folded heat exchanger with a flat heat exchanger.[1] This required the demolition of about one-fourth the tunnel loop and subsequent widening of

*Aerospace Engineer
†Aerospace Engineer, Senior Member AIAA
‡Mechanical Engineer

Copyright © 2001 by the American Institute of Aeronautics and Astronautics, Inc. No copyright is asserted in the United States under Title 17, U.S. Code. The U.S. Government has a royalty-free license to exercise all rights under the copyright claimed herein for Governmental Purposes. All other rights are reserved by the copyright owner.

[1] Actually, two flat exchangers were installed nearly side by side in the expanded tunnel loop. These two flat heat exchangers provided the same amount of cooling capacity as the original folded design, without the inherent degradation in tunnel flow quality. For simplicity, this set of heat exchangers will be referred to as the heat exchanger.

(c)2001 American Institute of Aeronautics & Astronautics or Published with Permission of Author(s) and/or Author(s)' Sponsoring Organization.

the tunnel shell to accept the larger flat heat exchanger. Figure 2 is a photograph of the new flat heat exchanger configuration. New corner turning vanes were installed upstream and downstream of the heat exchanger to insure an even distribution of airflow into and out of the heat exchanger leg of the tunnel.

A second major modification that impacted the tunnel flow quality was the installation of exit guide vanes (EGVs) downstream of the facility drive fan. Previous tests (Reference 1) indicated several flow quality concerns in the area downstream of the drive system, which were thought to be caused by the blockage of the drive motor housing support legs. The EGVs were designed to produce a more even flow field downstream of the fan. Improving the flow quality downstream of the fan was required to insure the best possible flow distribution into the heat exchanger.

As part of the recommissioning testing following the installation of these upgrades, flow quality surveys were conducted downstream of the fan drive motor housing and in the settling chamber upstream of the test section. The data from these surveys provided the information necessary to determine if the facility modifications were effective and could also be used to identify where further improvements might be made. This report documents all aspects of the tunnel loop flow quality surveys, and also provides a comparison to flow quality data collected prior to the facility modifications. The complete description of the IRT modifications is provided in References 2 through 6.

Description of Facility

The 6- by 9-foot Icing Research Tunnel (IRT) is a closed-loop atmospheric tunnel with rectangular cross sections. A 25-foot diameter twelve-blade fan that is powered by a 5000-hp electric motor drives the airflow. The tunnel, which has been in service since 1944, has undergone several major upgrades and modifications over the years to insure that it remains the premiere ground test facility for icing research. As mentioned, the tunnel was recently modified by replacing the original folded heat exchanger with a set of flat heat exchangers to improve both the aerodynamic flow quality and the icing cloud characteristics. To accommodate the new heat exchanger, the C-D leg of the tunnel loop was expanded. This also required new turning vanes to be installed in C and D corners. Exit guide vanes were also installed downstream of the fan to improve the flow quality entering the heat exchanger. The original tunnel layout is shown in Figure 3 and the new layout with the expanded C-D leg is shown in Figure 4.

The IRT test section is 6-ft high by 9-ft wide by 20-ft long. There is no divergence along any of the test section surfaces. The velocity in an empty test section can be varied between 50 and 390 mph (Mach numbers between 0.065 and 0.56) at 0°F.

Test Equipment

The test and support hardware as well as the data systems used during the tunnel loop flow quality surveys are described in the following sections.

Traversing Plates

To obtain velocity and pressure distribution data across the large sections of the tunnel (29.2 ft. wide by 26.2 ft. high), a traversing plate mechanism was used, as shown in Figure 5. The apparatus consists of a square channel[2] supported by cables at the leading and trailing edges. The cables are attached to channels that are mounted to the tunnel walls for horizontal surveys or the floor and ceiling for vertical surveys. The leading edge cable rides on a pulley that is driven by a remotely controlled electric motor so that the plate can be positioned at any point across the tunnel. The traverses were operated along both horizontal and vertical surveys. The traversing plates were used to collect data downstream of the fan drive motor and in the settling chamber. The traversing plates can support a variety of flow sensing probes; for these surveys, each traverse carried one pitot-static probe, one thermocouple, one hot wire anemometry probe and one wind anemometer (Figure 6). The selection of these flow probes provided not only a variety of measurements, but also added redundancy between some of the measurements. Three traverse mechanism and instrumentation sets were available for use, however only two were actually used, with the third held as a backup.

Instrumentation and Equipment

The following transducers and equipment were required to support the loop flow quality surveys:

- Pressure measurements: A 0 to 25 psia absolute pressure transducer was used to measure the total pressure measured by the pitot-static probes. A ±2.5-inches-of-water differential pressure transducer was used to measure the difference between total and static pressure.

[2] The traversing plate mechanisms were modified since the 1995 flow surveys test. The flat plates that originally carried the flow sensing probes were replaced with square channel. The square channel has a smaller profile so the air loads were reduced and therefore less likely to "fly", providing a more stable measurement platform. The basic operation of the traverses was not changed.

(c)2001 American Institute of Aeronautics & Astronautics or Published with Permission of Author(s) and/or Author(s)' Sponsoring Organization.

- Temperature measurements: An aspirated total temperature probe with a type "T" thermocouple was used.
- Wind anemometers: A frequency-to-DC converter was required for the propeller speed sensor (allows propeller rotational speed to be correlated to airspeed). A power supply was used to establish a voltage across the pitch and yaw potentiometers. The output of the propeller speed sensor and the output from the pitch and yaw potentiometers were recorded by Escort. The wind anemometers were calibrated in the NASA Glenn 3.5-inch diameter free jet facility for velocities ranging between 0 and 120 ft/sec and for pitch and yaw flow angles ranging between ±25°.
- Probe Actuation Control System (PACS): The PACS was used to control the motion and position of the traversing plates and to trigger data collection. This system consisted of a personal computer, 3 drive motors, 3 position/power/control units, and serial interface cables for communication with Escort.
- Hot wire anemometry: The hot wire measurements required a minimum of 4 hot wire anemometer units with integral signal conditioners, a personal computer with analog-to-digital converter data acquisition boards, data acquisition/reduction software, and a minimum of two hot wire X probes. The hot wire probes were fitted with 0.00015-inch diameter platinum coated tungsten wires.

Facility Instrumentation

The following standard facility instrumentation was used during this test program:

- Bellmouth/test section pitot-static probes: Two probes are mounted at the test section inlet, just downstream of the bellmouth, one on the inner wall and one on the outer wall. These probes are used to measure the test section total and static pressure.
- Total temperature probes in corner D: 24 total temperature type "T" thermocouple probes are arrayed on the turning vanes in corner D to measure the temperature profile exiting the facility cooler. The average of these 24 probes is used as the test section total temperature.

Steady-State Data Acquisition System

Real-time steady-state data acquisition and data display was provided by an Escort Alpha system. This system is the standard data acquisition and data display system used in the large test facilities at NASA Glenn. The system accommodates inputs from the Electronically Scanned Pressure System (ESP),[3] inputs from the facility distributed process control system, and inputs from any analog devices such as thermocouples and pressure transducers. This system recorded all steady-state pressures and temperatures from the traversing probes, the tunnel bellmouth pitot-static probes, and the facility total temperature probes. It also recorded important facility parameters such as fan rotational speed.

Existing Escort and post-processing programs for the loop flow quality surveys were used for these surveys (Escort program D033). The program had been converted to work on the new Escort Alpha operating platform. The Escort requirements and program were updated to include the increased number of C and D corner thermocouples. As part of the facility modifications, the number of thermocouples mounted in C and D corners was increased to provide a better means of monitoring and controlling the tunnel total temperature.

Hot Wire Instrumentation

Commercially available constant temperature anemometers were used for the hot wire turbulence intensity measurements. Four anemometers were used for the two dual sensor hot wire X probes. Each anemometer was equipped with its own signal conditioner for low-pass filtering, DC offsetting, and amplifying. Commercially available 12-bit personal computer based analog-to-digital converter data acquisition boards were used to digitize the hot wire signals. These boards had multiple input voltage ranges so that an optimal input range could be selected. This range was generally ±5 volts. A commercially available personal computer based graphical programming software package was used to build a customized hot wire data acquisition program with graphical user interface, data reduction/processing, and data archiving capabilities. This customized hot wire system was linked to the facility ESCORT and PACS systems so that data acquisition could be synchronously acquired with one trigger.

The hot wire probes were calibrated with a small bench top calibration jet supplied by a commercial vendor. The probes were calibrated for velocities ranging between 0 and 160 ft/sec and for flow angles ranging between ±30°. The nominal stagnation temperature during hot wire probe calibration was 75°F.

Test Matrix

Flow quality surveys consisting of pressure, airspeed, flow angle, and turbulence levels were made at two stations around the tunnel loop as shown in Figure 7. Downstream of the fan motor housing (station 2, vent tower door area), two horizontal and two vertical surveys were conducted. Upstream of the spray bars in the settling chamber, three horizontal and three vertical surveys were conducted.

[3] Since all pressure data were measured using individual transducers, the facility ESP system was not used during this test.

(c)2001 American Institute of Aeronautics & Astronautics or Published with Permission of Author(s) and/or Author(s)' Sponsoring Organization.

Data were collected as the traverses were moved from their starting points to the far end of the survey (outbound) and back to the starting point (return), thereby providing an opportunity to collect repeat data points as well as some data on the steadiness of the flow field as the data was collected at different times. The measurement interval was set to 6-inches for the outbound survey and 12-inches for the return survey. These surveys were conducted with an empty test section at a nominal test section airspeed of 350 mph. Previous tests have shown that there is little difference in loop flow quality with test section airspeed; therefore, only one test condition was used during these tests. The higher test section airspeed conditions produce higher airspeeds in the tunnel loop and this allows for better overall data quality and resolution. As the facility heat exchanger was not operational for these tests, all surveys were conducted at ambient temperature conditions.

Two test configurations were required to complete the two vertical and two horizontal surveys at the fan exit or in the vent tower area (station 2, see Figure 8):

1. Vertical surveys at the "inner" and "outer" locations ("inner" referring to survey closest to the inner wall and "outer" referring to the survey closest to the outer wall).
2. Horizontal surveys at the "floor" and "ceiling" locations ("floor" referring to the survey closest to the floor and "ceiling" referring to the survey closest to the ceiling).

Four test configurations were required to complete the three vertical and three horizontal surveys in the settling chamber just upstream of the spray bars (station 5, see Figure 8):

1. Vertical surveys at the "inner" and "centerline" locations.
2. Vertical surveys at the "centerline" and "outer" locations.
3. Horizontal surveys at the "floor" and "centerline" locations.
4. Horizontal surveys at the "centerline" and "ceiling" locations.

"Inner", "outer", "floor", and "ceiling" have the same meaning in the vent tower area. "Centerline" is self-explanatory.

Table 1 shows the test matrix for the tunnel loop flow quality survey testing based on the test conditions and configurations listed above.

Operational Procedures

Detailed written instructions were generated by the test engineering staff to aid the facility crew with test hardware installation and setup for each test run. The following are additional procedures that were specific to the loop flow quality survey tests.

1. The Test Engineer reviewed the test setup with the technicians prior to each run to insure that all hardware and instrumentation was properly installed.
2. Instrumentation continuity and leak checks were conducted following the initial installation and after each configuration change.
3. Detailed measurements were made of the test setup (positions of the traverses in the tunnel from convenient reference points).
4. Probe alignment measurements were made prior to each run as needed.
5. Detailed notes of the test setup and test execution were maintained in the Engineers Log Notebook.
6. At the start of each run, the operation of all instrumentation was checked through the Escort system. On-line data review continued throughout the run to insure the highest possible data quality.
7. Positioning of the cable traverse probes was controlled by PACS. A PACS profile was developed that moved the traverse to predetermined positions, allow for settling time, and triggered both Escort and hot wire data acquisition systems. This not only reduced the time required to complete the data collection, but also allows the test engineer to concentrate more on data review, thereby increasing that data quality. Each collected data reading was the average of ten to fifteen scans of data (scan rate of the Escort system was one scan per second).
8. The hot wire data acquisition system was setup to acquire data at a sampling rate of 4000 data points per second (4000 Hz) and to collect 32768 data points per channel. This works out to be 8.192 seconds worth of data. The low pass filters on the hot wire anemometer signal conditioners were set at 1000 Hz. These settings were adequate for the relatively low air velocities (20 to 60 ft/sec) in the vent tower and settling chamber areas.

There was one operational hurdle that was cleared during the loop flow quality testing, namely that the new facility heat exchanger was not yet operational, so it was not possible to set or control the tunnel temperature. Since the primary goal of the test was to determine the effects of the tunnel modifications on the aerodynamic

(c)2001 American Institute of Aeronautics & Astronautics or Published with Permission of Author(s) and/or Author(s)' Sponsoring Organization.

characteristics in the tunnel loop, it was felt that the testing could be completed without an operational heat exchanger, thereby helping to maintain the overall recommissioning schedule. The flow quality survey data were therefore collected while the tunnel temperature varied from about 50 to 90°F. The tunnel temperature was monitored during the surveys, to insure that the operating limits were not exceeded. Once the maximum allowable tunnel temperature was reached, the tunnel fan was dropped to idle and outside air was brought in through the vent tower to cool the tunnel. This limited test times to 10 to 20 minutes. Cooling required 20 to 40 minutes. While operating in this fashion was not very efficient from a testing standpoint, it did allow the test to be completed without delaying the overall recommissioning schedule.

Data Reduction and Analysis

The following sections describe the data reduction methodology, including corrections made to the data, which were used for this test.

Pressure/Air Speed Data

Local Mach number and airspeed at each traverse position was determined from the measured total and static pressure and total temperature. The Mach number was determined using the ratio of the static to total pressure and the isentropic perfect gas equation (equation 44 from reference 7 using γ=1.4)

$$M = \sqrt{5\left[\left(\frac{P_S}{P_T}\right)^{-0.2857} - 1\right]}$$

Velocity was determined using the definition of Mach number, $M = V/a$, where a is the speed of sound ($a = (\gamma R T_S)^{0.5}$). The static temperature, T_S, is calculated using the following relation (equation 43 from Reference 7).

$$T_S = \frac{T_T}{1 + 0.2 \cdot M^2}$$

The local velocity is then determined using

$$V = M \cdot a$$

Wind Anemometer Data

As previously mentioned, the wind anemometers were calibrated in a free jet. Linear curve fits resulted for air speed, pitch flow angle, and yaw flow angle versus output voltage. As a result, extracting engineering unit data from recorded wind anemometer output voltages was straightforward. There were a couple of anomalies in the wind anemometer data that had to be corrected. The first anomaly was with the air speed data for wind anemometer serial number 02. Electronic noise from some unknown source appeared in the propeller speed signal. Attempts to eliminate this noise were unsuccessful. As a result, the air speed indicated by this wind anemometer was high. To correct this problem, an in-situ calibration of this wind anemometer was performed using the adjacent pitot-static probe serial number 02 velocity as the standard. A linear curve fit was performed on these data and the results are shown in Figure 9. The curve-fit correction equation is given below.

$$V_{wa2,c} = 1.1663 \cdot V_{wa2} - 15.7291$$

$V_{wa2,c}$ is the corrected wind anemometer velocity in ft/sec and V_{wa2} is the original uncorrected wind anemometer velocity in ft/sec.

The second anomaly required that the wind anemometer pitch angle data from the horizontal ceiling (elevation of 234 inches above the floor) and horizontal floor (75.5 inches above the floor) surveys in the settling chamber be corrected. The data were biased in the negative pitch direction when compared to pitch data from the settling chamber vertical surveys. The horizontal ceiling and floor survey data were shifted in the positive pitch direction so that the pitch angles would closely match the data from the vertical surveys at the same elevation. The ceiling data were shifted by +7.72 degrees and the floor data were shifted by +8.66 degrees. The shape of the profiles remained the same (just shifted upward). These data corrections were viewed as acceptable since it was noticed during testing that the traverse instrumentation may have sagged or pitched downward due to gravity as the instrumentation approached the center position. It is unfortunate that actual "sag" angles were not quantified. It must be emphasized that only the pitch angle data from these two horizontal surveys were corrected.

Turbulence Intensity Data

As previously mentioned, hot wire probes were calibrated prior to being used in the IRT. Dual sensor hot wire X probes were used exclusively for this test. For these probes, two calibration curves are required (one curve for each sensor). Third order polynomials were satisfactory in fitting the effective velocity data $V_{HW,cal,eff,i}$ to the hot wire anemometer bridge voltage, $E_{HW,cal,i}$. The equations below describe the calibration curve fit process.

$$V_{HW,cal,eff,i} = V_{jet,cal} \cdot \cos(\alpha_{HW,cal} + \theta_{HW,i})$$

(c)2001 American Institute of Aeronautics & Astronautics or Published with Permission of Author(s) and/or Author(s)' Sponsoring Organization.

$$V_{HW,cal,eff,i} = a_i + b_i \cdot E_{HW,cal,i} + c_i \cdot E^2_{HW,cal,i} + d_i \cdot E^3_{HW,cal,i}$$

where $i = 1$ for the first X probe sensor and $i = 2$ for the second X probe sensor. $\theta_{HW,i}$ is the sensor angle relative to the freestream velocity vector when the hot wire probe angle of attack, $\alpha_{HW,cal}$ is 0°. For all of the hot wire X probes used, $\theta_{HW,1}$ = +45° and $\theta_{HW,2}$ = –45°. During calibration $\alpha_{HW,cal}$ varies between ±30°. For the hot wire probes used, all of the data for one sensor collapsed down to one curve regardless of $V_{jet,cal}$ and $\alpha_{HW,cal}$. The idea is to have an increase in $E_{HW,cal,i}$ be correlated with an increase in $V_{HW,cal,eff,i}$ and vice-verse for both sensors regardless of $\alpha_{HW,cal}$. Hot wire probe calibration was typically carried out at a total temperature of about 75°F.

Once the calibration curve fit coefficients are available for the calibration data, an equation from Reference 8 is used to correct the hot wire anemometer bridge output voltages for deviations in test total temperature from the calibration total temperature.

$$E_{HW,test,i,c} = E_{HW,test,i} \cdot \sqrt{\frac{(T_{T,sensor} - T_{T,cal})}{(T_{T,sensor} - T_{T,test})}}$$

The value of $T_{T,sensor}$ used was 482 °F. $T_{T,cal}$ was typically 75 °F and $T_{T,test}$ varied between 50 and 90 °F.

At this point, the polynomial calibration coefficients, a_i, b_i, c_i, and d_i and the corrected hot wire anemometer bridge output voltages, $E_{HW,test,i,c}$, can be used to compute test effective velocities, $V_{HW,eff,i}$. A correction to these effective velocities is applied to compensate for changes in static pressure from calibration to test. The correction equation is taken from Reference 8 and is given below.

$$V_{HW,eff,i,c} = V_{HW,eff,i} \cdot \frac{P_{S,cal}}{P_{S,test}}$$

Hot wire velocity vector magnitude is given by the equation below.

$$V_{HW} = \sqrt{V^2_{HW,eff,1,c} + V^2_{HW,eff,2,c}}$$

As hot wire data reduction was progressing, it was noted from data plots that hot wire velocity vectors lost about 0.30303 ft/sec in magnitude for every 1°R increase in temperature compared to the pitot-static velocities. For this reason, one final empirical correction was applied to the velocity vector magnitude as seen below.

$$V_{HW,c} = V_{HW} + 0.30303 \cdot (T_{T,test} - T_{T,cal})$$

Hot wire flow angles and velocity components were finally computed with the following equations.

$$\alpha_{HW} = 45^\circ - \tan^{-1}\left(\frac{V_{HW,eff,2,c}}{V_{HW,eff,1,c}}\right)$$

$$u_{HW} = V_{HW,c} \cdot \cos(\alpha_{HW})$$

$$v_{HW} = V_{HW,c} \cdot \sin(\alpha_{HW})$$

Mean, standard deviation, and turbulence intensity follow with the equations below. The value of N used was 32768.

$$u_{HW,avg} = \frac{1}{N}\sum_{j=1}^{N} u_{HW,j}$$

$$v_{HW,avg} = \frac{1}{N}\sum_{j=1}^{N} v_{HW,j}$$

$$V_{HW,avg} = \sqrt{u^2_{HW,avg} + v^2_{HW,avg}}$$

$$\sigma_{u_{HW}} = \sqrt{\frac{1}{N-1}\sum_{j=1}^{N}\left(u_{HW,j} - u_{HW,avg}\right)^2}$$

$$\sigma_{v_{HW}} = \sqrt{\frac{1}{N-1}\sum_{j=1}^{N}\left(v_{HW,j} - v_{HW,avg}\right)^2}$$

$$TI_u = \frac{\sigma_{u_{HW}}}{V_{HW,avg}} \times 100\%$$

$$TI_v = \frac{\sigma_{v_{HW}}}{V_{HW,avg}} \times 100\%$$

More information about hot wire anemometry can be found in Reference 9.

(c)2001 American Institute of Aeronautics & Astronautics or Published with Permission of Author(s) and/or Author(s)' Sponsoring Organization.

Discussion of Results

Table 2 is a summary of the data readings collected for each test configuration during 1995 and 2000 that were used in this data discussion. Table 3 is a statistical summary of all flow quality results from the years 1995 and 2000 for the vent tower area and settling chamber in terms of mean and standard deviation. The mean and standard deviation numbers in this table were computed by assembling all of the appropriate horizontal and vertical profiles and calculating the mean and standard deviation of this assembled profile grouping. The percent change numbers were computed as follows:

$$Change = \frac{2000Parameter - 1995Parameter}{1995Parameter} \cdot 100\%$$

The pitch and yaw flow angle percent change numbers were computed using the same equation except that absolute values of the parameters were used. A column of estimated measurement uncertainty is provided so that the reader can judge the relative validity of individual improvements or degradations. Referring to this table while reviewing the data plots will assist in quantifying the precise levels of improvement or degradation.

All of the loop flow quality data acquired in 2000 were obtained at a test section air speed of 350 mph. The data from 1995 was also obtained at this same test section air speed. In 1995, the data were acquired at a tunnel stagnation temperature of 40°F ± 5°F. In 2000, the data were acquired with the stagnation temperature varying between 50°F and 95°F. For this reason, no comparison of temperature distributions will be made.

When flow angles are discussed, the sign convention is as follows: positive (+) pitch indicates flow toward the ceiling, negative (–) pitch indicates flow toward the floor, positive (+) yaw indicates flow toward the outer wall, and negative (–) yaw indicates flow toward the inner wall.

Vent Tower Area

At the fan exit, exit guide vanes (EGVs) were installed to make the velocity distribution more uniform so that the new flat heat exchanger would have uniform flow at its inlet face. The 1995 data showed two areas of concern downstream of the fan. First was a high-speed region near the floor directly downstream of the drive motor housing. The second was a very low speed region near the outside tunnel wall. These problem areas were caused by the blockage of the drive motor housing supports. The EGVs were added to evenly distribute the blockage and thereby produce a uniform flow field. Figures 10 and 11 show horizontal and vertical velocity profiles for the vent tower area. Shown are data from the pitot-static pressure probes, wind anemometers, and hot wire probes for the years 2000 and 1995. It is apparent that the EGVs were successful in making the velocity profiles more uniform and flat (particularly the horizontal profiles). There was roughly a 30.5% reduction in the standard deviation of the pitot-static velocity profiles and a 6.3% reduction in the mean of the pitot-static velocity profiles. Data from the wind anemometer and hot wire probes were similar. It is not exactly clear why there was a reduction in the mean if the test section air speed remained the same. It may be that 4 profiles were not enough to accurately measure the mean velocity of such a large area.

Figures 12 and 13 show the horizontal and vertical turbulence intensity profiles for the vent tower area. Shown are axial and transverse (horizontal or vertical) turbulence intensities for the years 2000 and 1995. There was a 7.4% and a 19.6% reduction in the axial turbulence intensity profile mean and profile standard deviation respectively. There was an 11.8% increase and a 2.1% reduction in the transverse turbulence intensity profile mean and profile standard deviation respectively. When the actual numbers are compared and the data plots are inspected, it is apparent that these changes are very minimal. It appears that the outlet guide vanes did not improve the unsteadiness or turbulence in the vent tower area. The authors did witness very turbulent and "choppy" airflow in the vent tower area by observing the cable traverse hardware motion with remote cameras.

Figures 14 and 15 show the horizontal and vertical pitch and yaw flow angle profiles for the vent tower area. Shown are data from the wind anemometers and the hot wire probes for the years 2000 and 1995. There was a 34.6% reduction and a 19.2% increase in the wind anemometer pitch flow angle profile mean and profile standard deviation respectively. There was an 81.5% reduction and a 14.9 percent increase in the hot wire pitch flow angle profile mean and profile standard deviation respectively. The wind anemometer yaw flow angle profiles registered a 49.5% increase in the profile mean and a 29.2% reduction in the profile standard deviation. The hot wire yaw flow angle profiles registered a 491.7% (+1.07° to –6.33°) increase in the profile mean and a 37.5% reduction in the profile standard deviation. When reviewing the data plots and the absolute statistical numbers in Table 2, it is apparent that the percent change numbers may be misleading and that all of the data generally lie within ±10 degrees. There do not appear to be any strong trends of improvement or degradation. Keep in mind that the purpose of the fan outlet guide vanes was to make the velocity profiles more uniform and not necessarily improve turbulence intensity or flow angle.

(c)2001 American Institute of Aeronautics & Astronautics or Published with Permission of Author(s) and/or Author(s)' Sponsoring Organization.

Settling Chamber

The replacement of the original folded heat exchanger with a pair of flat heat exchangers was expected to have a significant impact on the flow quality in the settling chamber, which in turn would lead to improved test section flow quality. The 1995 data showed that the folded heat exchanger included significant nonuniformities in all flow quality parameters (pressure, airspeed, flow angle and turbulence). Replacing the folded heat exchanger with the flat heat exchanger not only removed the cause of these nonuniformities, but the flat heat exchanger does in fact act as a flow conditioning device in that its uniform pressure drop aids in evenly distributing the flow within the tunnel shell.

Figures 16 and 17 show the horizontal and vertical velocity profiles for the IRT settling chamber. Shown are data from the pitot-static pressure probes, the wind anemometers, and the hot wire probes for years 2000 and 1995. It is very apparent from these plots that the combination of the fan outlet guide vanes, the new turning vanes, and the new flat heat exchangers dramatically improved the quality of the velocity profiles in the settling chamber. All three probes registered about an 83% improvement in the velocity profile standard deviation. The pitot-static velocity profiles registered a 3.2% or a 1.1 ft/sec reduction in profile mean. This indicated reduction in profile mean might be a result of the surveying such a large area with only 6 linear traverses.

Figures 18 and 19 show horizontal and vertical turbulence intensity profiles for the IRT settling chamber. Shown are axial and transverse (horizontal or vertical) turbulence intensity profiles for years 2000 and 1995. It is apparent from the plots that the turbulence intensity has been significantly reduced. The axial turbulence intensity profile mean was reduced by 68.7% and the profile standard deviation was reduced by 79.9%. The transverse turbulence intensity profile mean was reduced by 50.0% and the profile standard deviation was reduced by 58.6%.

Figures 20 and 21 show horizontal and vertical profiles of pitch and yaw flow angle for the IRT settling chamber. Flow angle data from wind anemometer and hot wire probes are shown for years 2000 and 1995. The wind anemometer and hot wire probes registered a 73.6% and a 77.0% reduction in the pitch flow angle profile mean respectively. They also showed a 49.1% reduction and 47.5% increase in pitch flow angle profile standard deviation respectively. The wind anemometer and the hot wire probes measured a 58.2% increase and a 50.0% decrease in yaw angle profile mean respectively. They also measured a 10.0% and a 30.7% reduction in yaw profile standard deviation. Overall, the flow angle picture was improved. The two exceptions are not very significant since the changes were less than one degree. In essence, the improved flow angles validate the turning vane design and installation.

Summary of Results

The 1999 Icing Research Tunnel Facility modifications including new fan outlet guide vanes, new C and D corner turning vanes, and new flat heat exchangers resulted in the following flow quality improvements when compared to the 1995 baseline flow quality measurements:

- 30.5% reduction in vent tower velocity profile standard deviation
- Three of the four vent tower turbulence intensity statistics saw improvements
- Four of the eight vent tower flow angle statistics saw improvements
- 82.0% reduction in settling chamber velocity profile standard deviation
- 68.7% reduction in settling chamber axial turbulence intensity profile mean
- 79.9% reduction in settling chamber axial turbulence intensity profile standard deviation
- 50.0% reduction in settling chamber transverse turbulence intensity profile mean
- 58.6% reduction in settling chamber transverse turbulence intensity profile standard deviation
- Six of the eight settling chamber flow angle statistics saw improvements

Concluding Remarks

A series of surveys were conducted in the NASA Glenn Icing Research Tunnel to ascertain the impact of major facility modifications on the overall flow quality. This report described in detail the hardware, instrumentation, test procedures, data and results from these surveys. While the tests were successfully completed and the results indicated that the flow quality in the IRT loop was improved by the facility modifications, there were some lessons learned and recommendations generated for consideration:

- Direct on-line measurements of the traversing plate angles of incidence should be made to reduce the uncertainty in flow angle measurements.
- Install larger propellers on the wind anemometers. This will allow the measurement of slower air velocities. Model airplane propellers should be considered.

(c)2001 American Institute of Aeronautics & Astronautics or Published with Permission of Author(s) and/or Author(s)' Sponsoring Organization.

- New motors were purchased to drive the traverses, however they were not powerful enough to drive the probes, brackets, and instrumentation cabling up to the needed elevations. New gear heads (5:1) were purchased to provide a better power ratio. However, the problem was solved without the new parts by counterbalancing the traverse (that is a weight was used to counter the plate and instrumentation). The traverse gearing should be corrected so that the motors can drive the plates vertically, thereby eliminating the need for the counterweights (the weights could interfere with the movement of the instrumentation lines). Before using the cable traverse systems again, a thorough checkout of the hardware using the 5:1 gear heads with all of the instrumentation cable weight should be performed. Also, smaller and lighter electric cable should be used for the wind anemometers to further reduce the overall weight of the system.

References

1. Arrington, E.A., Gonsalez, J.C., and Kee-Bowling, B.A.: Flow Quality Studies of the NASA Glenn Research Center Icing Research Tunnel Circuit (1995 Tests), NASA/TM—2000-107479, March 2000.
2. Irvine, T., Kevdzija, S., Sheldon, D., and Spera, D.: Overview of the NASA Glenn Icing research Tunnel Icing and Flow Quality Improvements Program. AIAA paper 2001–0229, January 2001.
3. Canacci, V.A., Gonsalez, J.C., and Spera, D.A.: Use of a Scale Model tunnel in the Design of Facility Modification for the NASA Glenn Icing Research Tunnel. AIAA paper 2001–0230, January 2001.
4. Sheldon, D., Andrachio, C., Krivanek, T. Spera, D., and Austinson, T.: Lessons Learned and Results from the Construction Phase and Qualification Testing of the Icing Research Tunnel. AIAA paper 2001–0231, January 2001.
5. Gonsalez, J.C., Arrington, E.A., and Curry, III, M.R.: Aero-Thermal Calibration of the NASA Glenn Icing Research Tunnel (2000 Tests). AIAA paper 2001–0233, January 2001.
6. Ide, R. and Oldenberg, J.: Icing Cloud Calibration of the NASA Glenn Icing Research Tunnel. AIAA paper 2001–0234, January 2001.
7. Ames Aeronautical Laboratory: Equations, Tables and Charts for Compressible Flow. NACA TR–1135 (NASA TN–1428), 1953.
8. "TSI Model DAP IFA Thermal Anemometry Software Package, Instruction Manual", TSI Incorporated, St. Paul, MN, Revision A, January 1993.
9. Bruun, H.H.: Hot–Wire Anemometry, Principles and Signal Analysis, Oxford University Press, 1995.

(c)2001 American Institute of Aeronautics & Astronautics or Published with Permission of Author(s) and/or Author(s)' Sponsoring Organization.

Table 1.—Test matrix for the January 2000 IRT loop flow quality survey tests.

Station	Traverse Configuration	Traverse Positions	Test Section Airspeed, mph	Tunnel Total Temperature
2	1	Inner, Outer	350	ambient
2	2	Floor, Ceiling	350	ambient
5	1	Inner, Centerline	350	ambient
5	2	Centerline, Outer	350	ambient
5	3	Floor, Centerline	350	ambient
5	4	Centerline, Ceiling	350	ambient

Table 2.—Data Archive Information from the 1995 and 2000 IRT Loop Flow Quality Surveys.

Date	Data Readings (pgm D033)	Location	Traverse Orientation	Traverse 1 Position[a]	Traverse 2 Position[a]	Test section air speed (mph)
2/21/95	0711-0759	Settling chamber	Vertical	87.8 (Inner)	195.5 (Center)	350
2/22/95	0991-1040	Settling chamber	Vertical	263.0 (Outer)	(Not used)	350
2/23/95	1265-1308	Settling chamber	Horizontal	72.5 (Floor)	156.0 (Center)	350
4/18/95	1480-1515	Settling chamber	Horizontal	156.0 (Center)	234 (Ceiling)	350
4/25/95	1883-1933	Vent tower	Vertical	111.0 (Inner)	224.0 (Outer)	350
4/26/95	2098-2147	Vent tower	Horizontal	204.0 (Ceiling)	102.5 (Floor)	350
1/13/00	2752-2857	Vent tower	Vertical	111.0 (Inner)	224.0 (Outer)	350
1/18/00	2858-2939	Vent tower	Horizontal	102.5 (Floor)	204.0 (Ceiling)	350
1/20/00	2940-3076	Settling chamber	Horizontal	156.0 (Center)	234 (Ceiling)	350
1/21/00	3077-3212	Settling chamber	Horizontal	156.0 (Center)	72.5 (Floor)	350
1/25/00	3213-3329	Settling chamber	Vertical	87.7 (Inner)	195.5 (Center)	350
1/26/00	3330-3463	Settling chamber	Vertical	263.0 (Outer)	195.5 (Center)	350

[a] Vertically oriented traverse positions are referenced from the tunnel inner wall; horizontally oriented traverse positions are referenced from the floor..

(c)2001 American Institute of Aeronautics & Astronautics or Published with Permission of Author(s) and/or Author(s)' Sponsoring Organization.

Table 3.—Summary of statistical results from 1995 and 2000 IRT flow quality surveys in the vent tower area and settling chamber.

Survey Location	Parameter	Probe	Statistical Quantity	Units	Estimated Uncert.	1995	2000	Change	Comment
Vent tower	Velocity	Pitot-static	Mean	ft/sec	±0.5	34.99	32.78	-6.3%	
			Std. dev.	ft/sec	±0.5	12.30	8.55	-30.5%	Improvement
		Wind anem.	Mean	ft/sec	±0.5	33.10	30.02	-9.3%	
			Std. dev.	ft/sec	±0.5	12.19	9.31	-23.6%	Improvement
		Hot wire	Mean	ft/sec	±0.5	37.39	32.74	-12.4%	
			Std. dev.	ft/sec	±0.5	12.38	8.60	-30.5%	Improvement
	Axial turbulence intensity	Hot wire	Mean	%	±0.5	24.48	22.67	-7.4%	Improvement
			Std. dev.	%	±0.5	5.67	4.56	-19.6%	Improvement
	Transverse turbulence intensity	Hot wire	Mean	%	±0.5	19.25	21.52	11.8%	Degradation
			Std. dev.	%	±0.5	4.00	3.91	-2.1%	Improvement
	Pitch flow angle	Wind anem.	Mean	degrees	±1	2.34	-1.53	-34.6%	Improvement
			Std. dev.	degrees	±1	4.32	5.15	19.2%	Degradation
		Hot wire	Mean	degrees	±1	3.00	-0.55	-81.5%	Improvement
			Std. dev.	degrees	±1	2.32	2.67	14.9%	Degradation
	Yaw flow angle	Wind anem.	Mean	degrees	±1	0.06	0.09	49.5%	Degradation
			Std. dev.	degrees	±1	7.10	5.02	-29.2%	Improvement
		Hot wire	Mean	degrees	±1	1.07	-6.33	491.7%	Degradation
			Std. dev.	degrees	±1	3.09	1.93	-37.5%	Improvement
Settling Chamber	Velocity	Pitot-static	Mean	ft/sec	±0.5	35.25	34.11	-3.2%	
			Std. dev.	ft/sec	±0.5	8.31	1.50	-82.0%	Improvement
		Wind anem.	Mean	ft/sec	±0.5	32.01	33.45	4.5%	
			Std. dev.	ft/sec	±0.5	8.84	1.46	-83.5%	Improvement
		Hot wire	Mean	ft/sec	±0.5	37.38	34.27	-8.3%	
			Std. dev.	ft/sec	±0.5	8.05	1.37	-83.0%	Improvement
	Axial turbulence intensity	Hot wire	Mean	%	±0.5	8.38	2.62	-68.7%	Improvement
			Std. dev.	%	±0.5	3.40	0.68	-79.9%	Improvement
	Transverse turbulence intensity	Hot wire	Mean	%	±0.5	6.29	3.15	-50.0%	Improvement
			Std. dev.	%	±0.5	2.26	0.94	-58.6%	Improvement
	Pitch flow angle	Wind anem.	Mean	degrees	±1	3.40	0.90	-73.6%	Improvement
			Std. dev.	degrees	±1	3.78	1.92	-49.1%	Improvement
		Hot wire	Mean	degrees	±1	2.67	0.61	-77.0%	Improvement
			Std. dev.	degrees	±1	0.96	1.42	47.5%	Degradation
	Yaw flow angle	Wind anem.	Mean	degrees	±1	-0.32	0.50	58.2%	Degradation
			Std. dev.	degrees	±1	2.92	2.63	-10.0%	Improvement
		Hot wire	Mean	degrees	±1	-2.26	1.13	-50.0%	Improvement
			Std. dev.	degrees	±1	3.54	2.45	-30.7%	Improvement

(c)2001 American Institute of Aeronautics & Astronautics or Published with Permission of Author(s) and/or Author(s)' Sponsoring Organization.

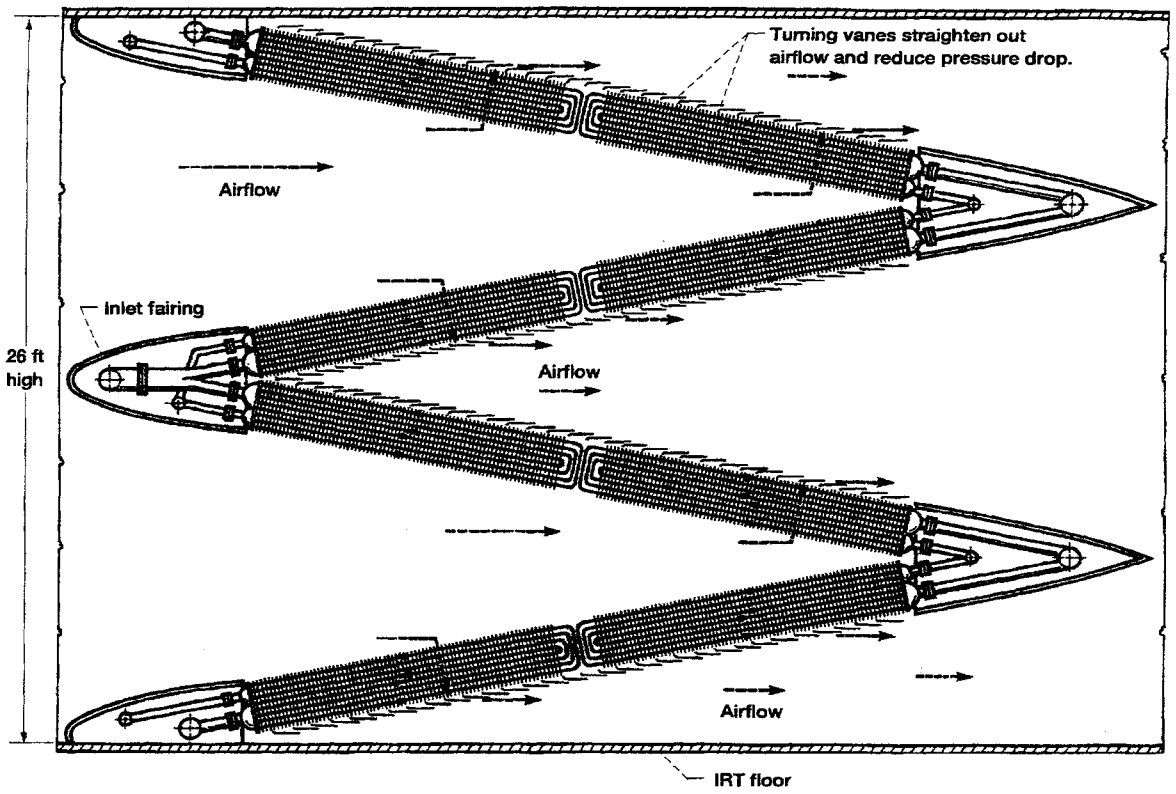

Figure 1.—Elevation view of the original IRT folded heat exchanger.

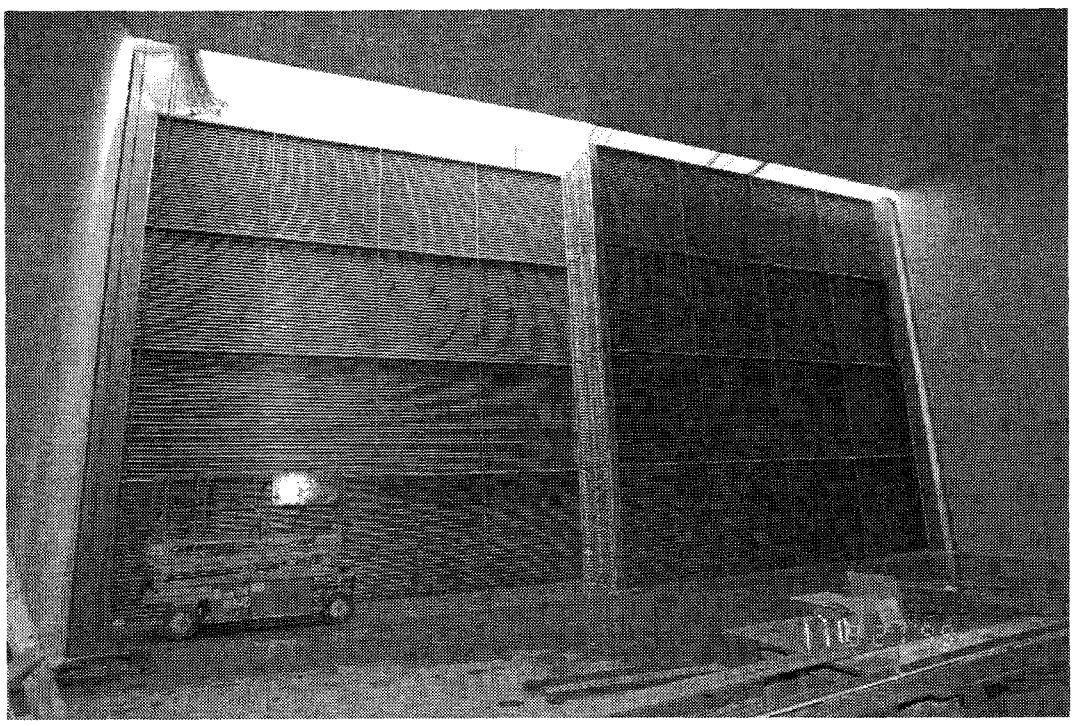

Figure 2.—Installation photograph of the new IRT flat heat exchanger.

(c)2001 American Institute of Aeronautics & Astronautics or Published with Permission of Author(s) and/or Author(s)' Sponsoring Organization.

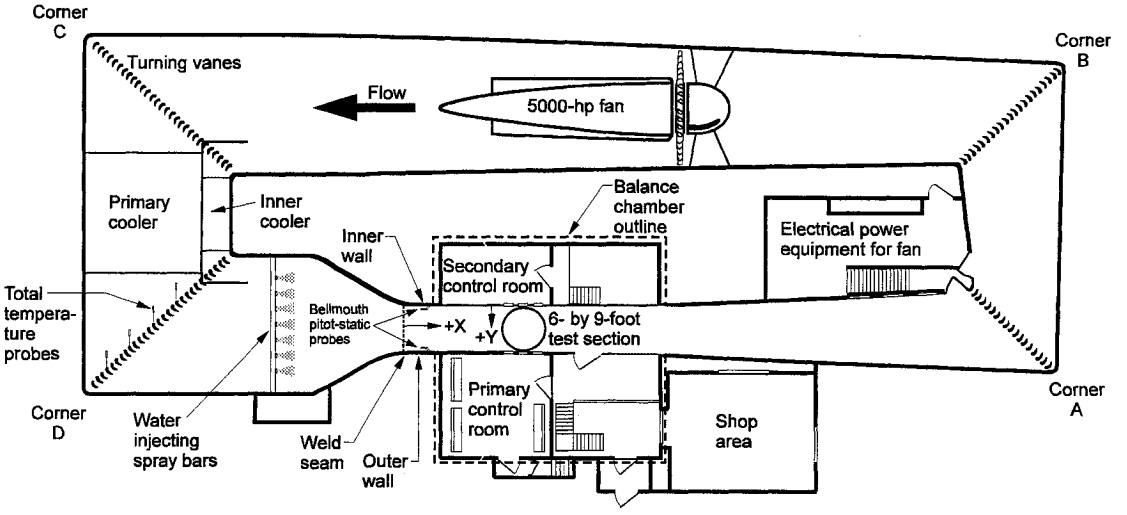

Figure 3.—Layout of the NASA Glenn Icing Research Tunnel prior to the replacement of the folded heat exchanger.

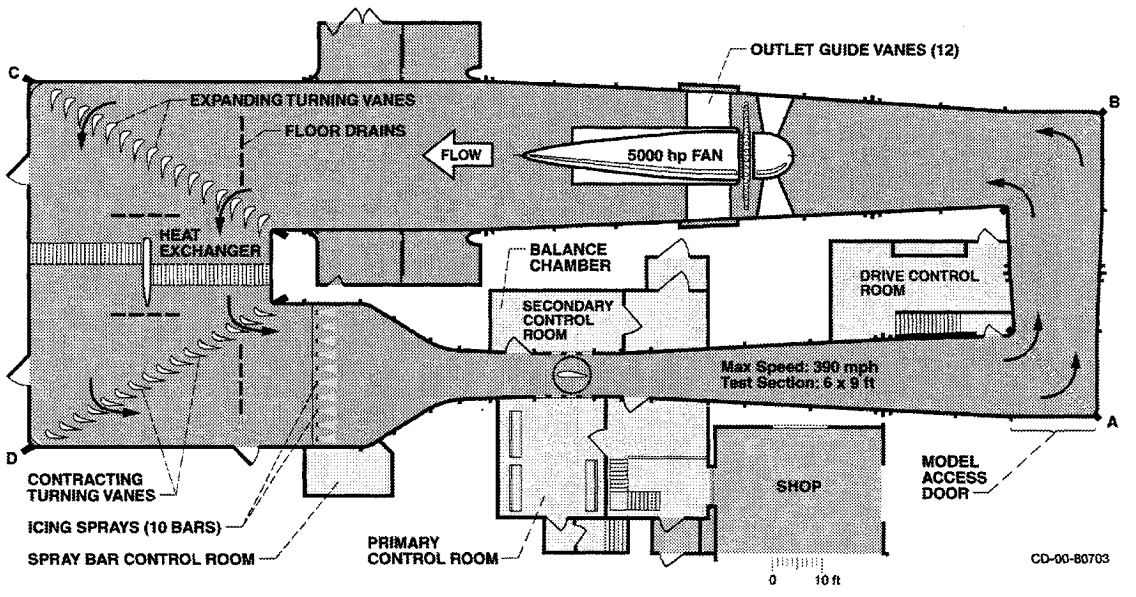

Figure 4.—Layout of the NASA Glenn Icing Research Tunnel following replacement of the original folded heat exchanger with a pair of flat heat exchangers. The C-D leg of the tunnel loop was expanded to accommodate the width of the flat heat exchangers. Exit guide vanes were also installed downstream of the drive fan.

(c)2001 American Institute of Aeronautics & Astronautics or Published with Permission of Author(s) and/or Author(s)' Sponsoring Organization.

(a)

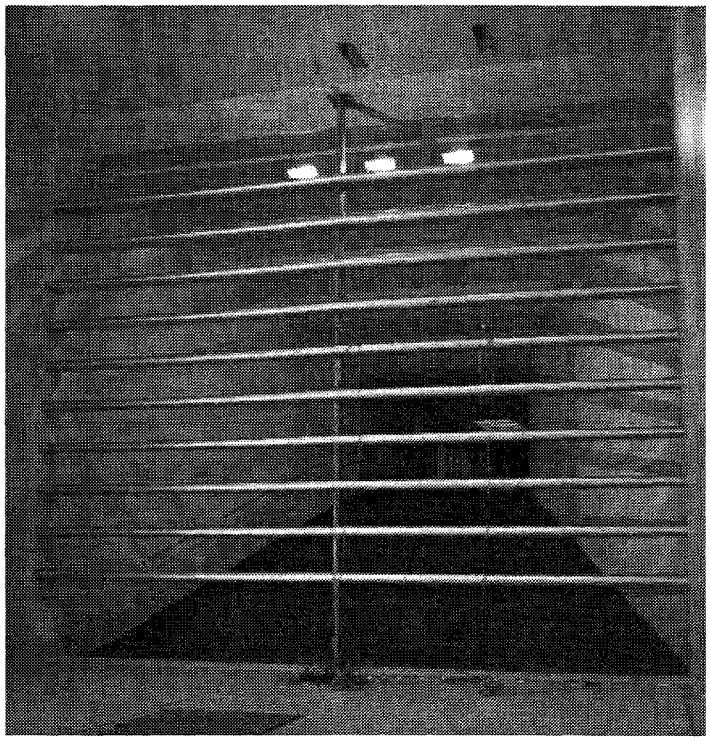

(b)

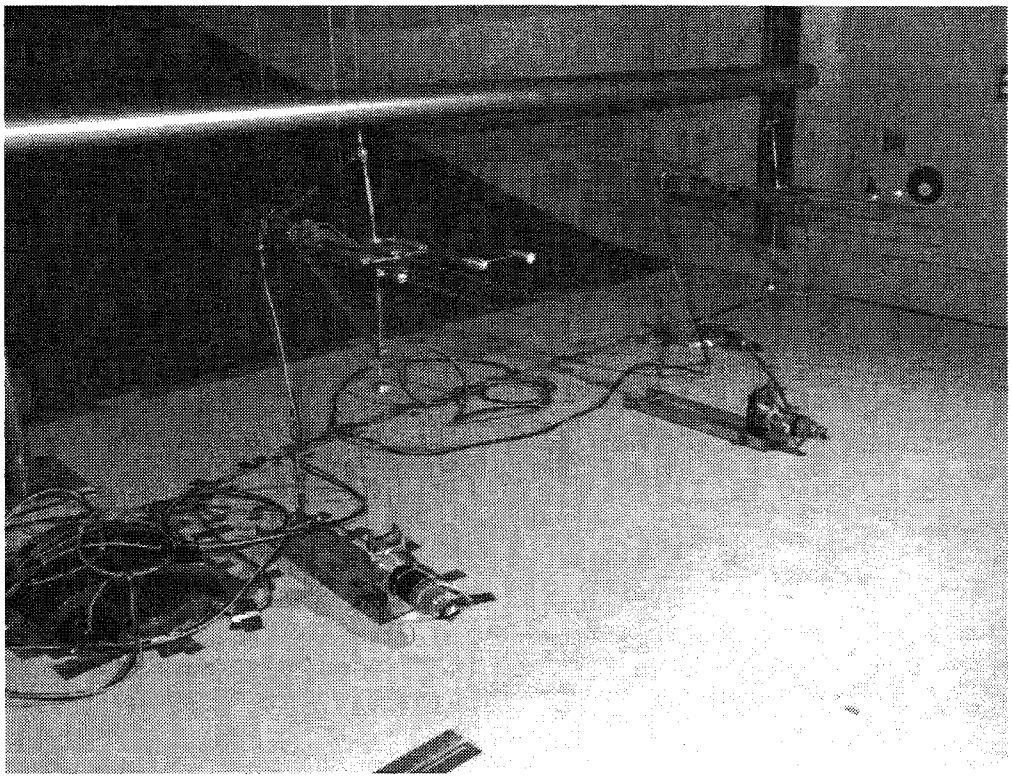

Figure 5.—Typical installation of the traversing plate mechanisms in the settling chamber of the Icing Research Tunnel. (a) View of two vertical traverses mechanisms in the settling chamber. (b) Detail of plate mounting, motors and instrumentation.

(c)2001 American Institute of Aeronautics & Astronautics or Published with Permission of Author(s) and/or Author(s)' Sponsoring Organization.

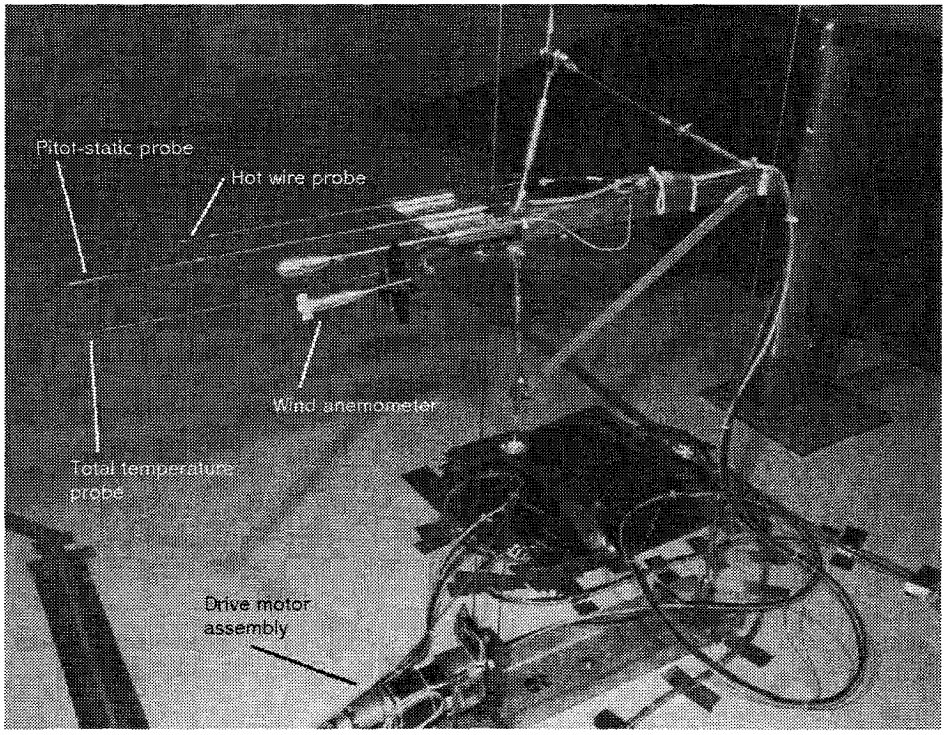

Figure 6.—Close-up view of a traversing mechanism showing the instrumentation used during the IRT loop flow quality surveys.

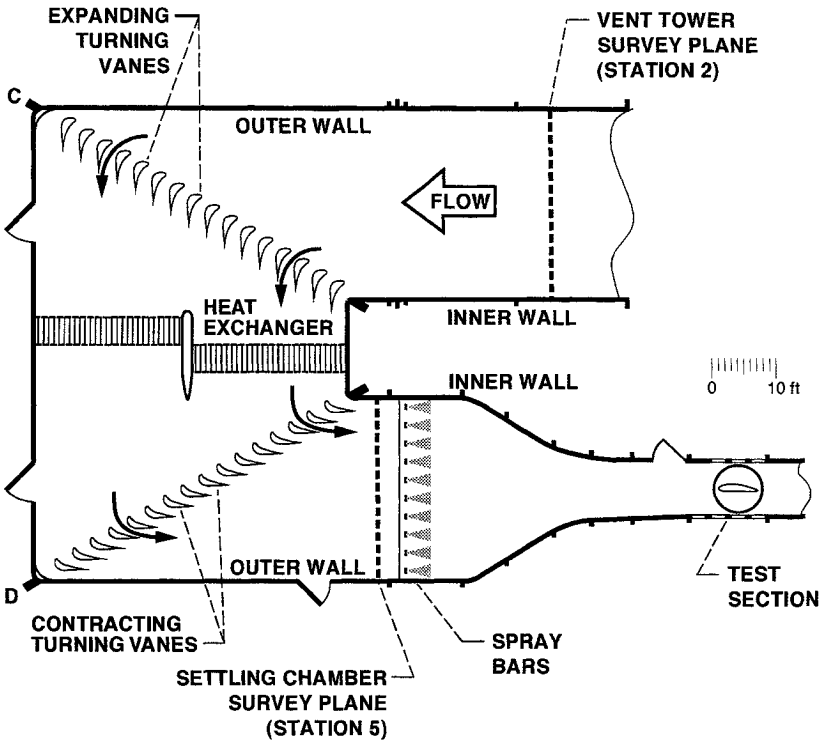

Figure 7.—Planview of the modified Icing Research Tunnel C-D leg showing the locations of flow quality surveys.

(c)2001 American Institute of Aeronautics & Astronautics or Published with Permission of Author(s) and/or Author(s)' Sponsoring Organization.

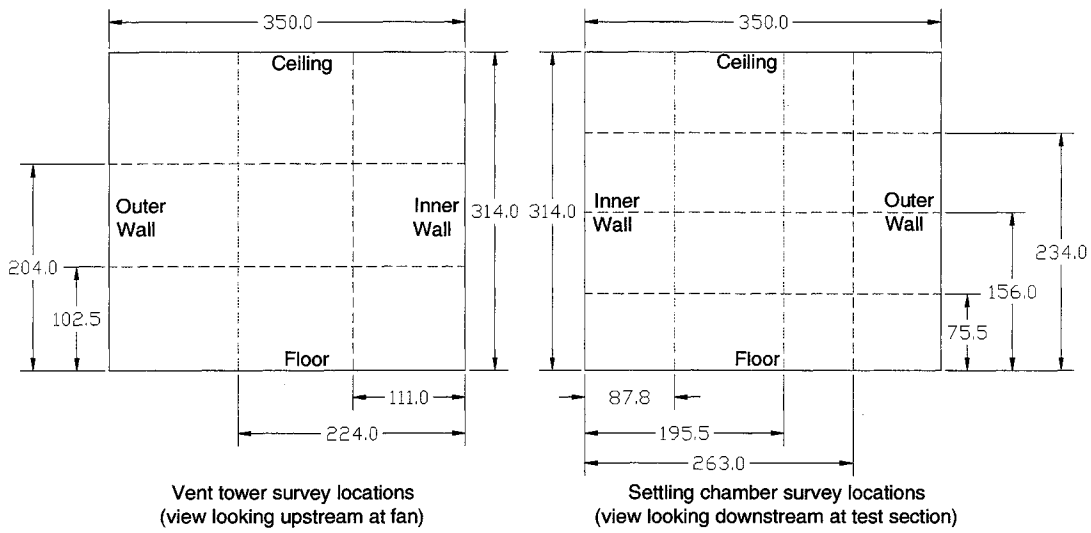

Figure 8.—Horizontal and vertical flow quality survey locations in the IRT vent tower and settling chamber. All dimensions are in inches. Locations are applicable to both 1995 and 2000 surveys.

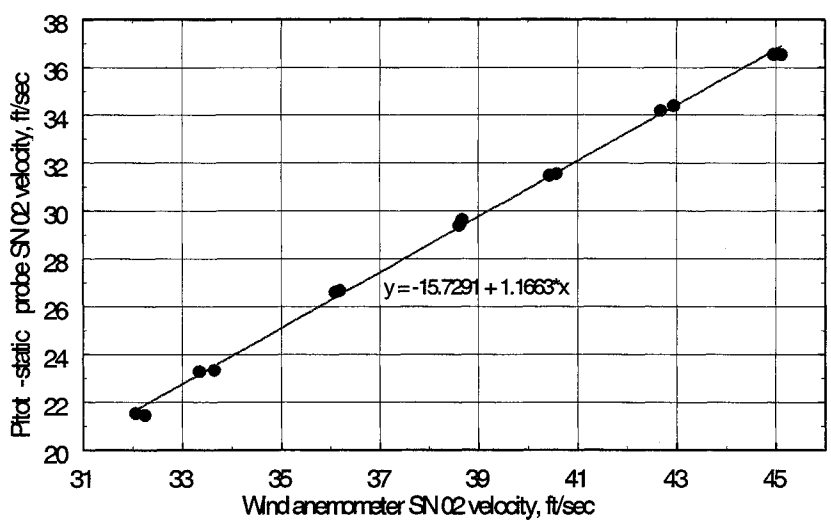

Figure 9.—Plot illustrating in-situ calibration of IRT wind anemometer serial number 02.

(c)2001 American Institute of Aeronautics & Astronautics or Published with Permission of Author(s) and/or Author(s)' Sponsoring Organization.

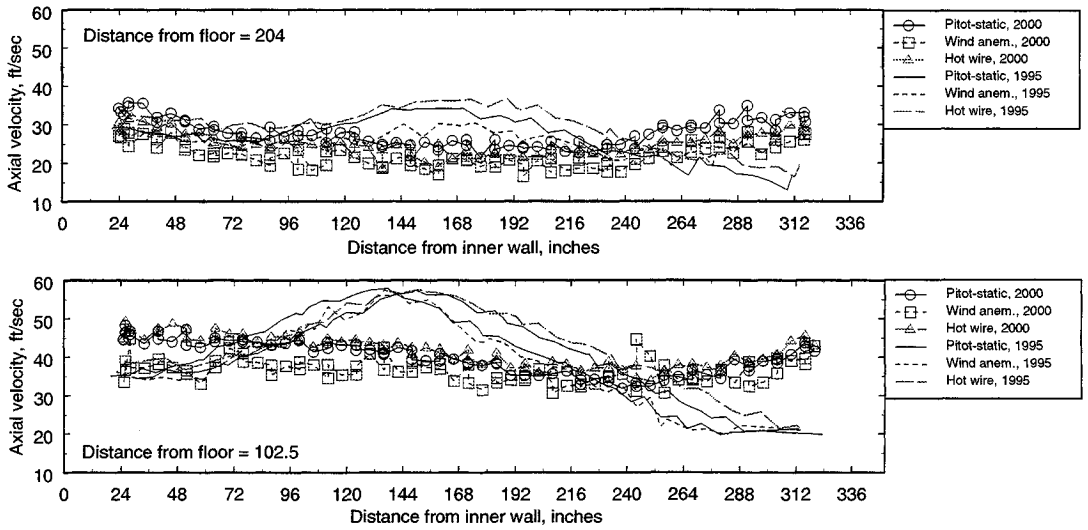

Figure 10.—Horizontal velocity profiles in the IRT vent tower area.

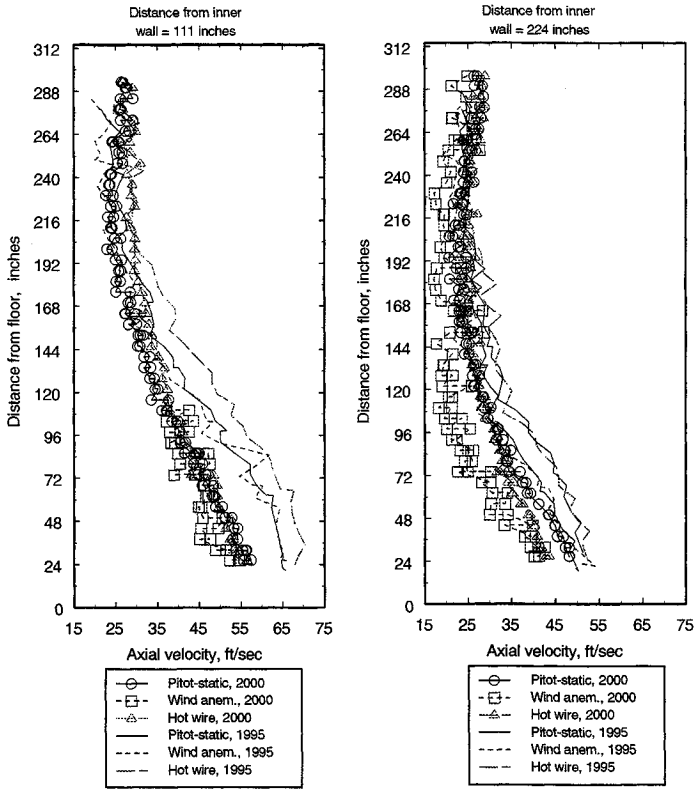

Figure 11.—Vertical velocity profiles in the IRT vent tower area.

(c)2001 American Institute of Aeronautics & Astronautics or Published with Permission of Author(s) and/or Author(s)' Sponsoring Organization.

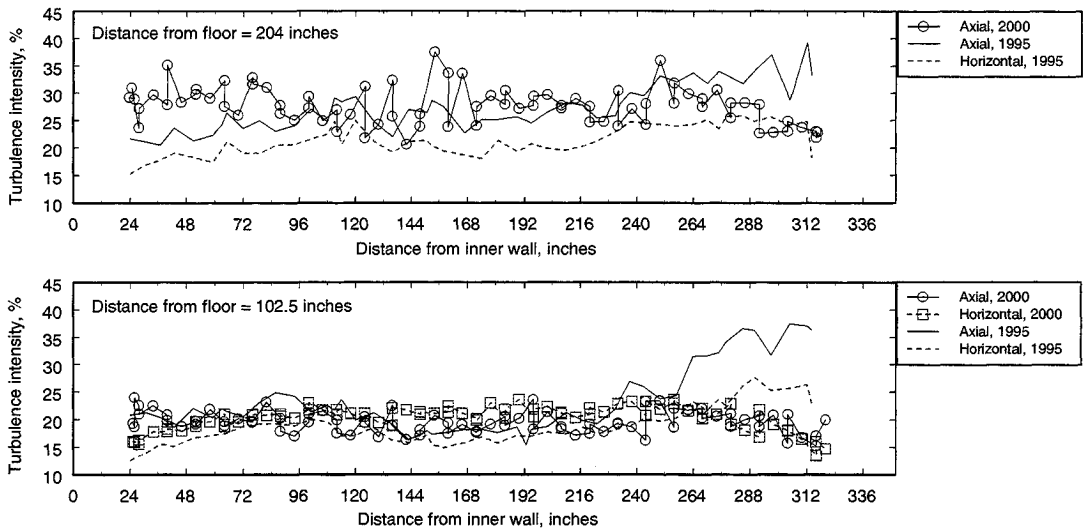

Figure 12.—Horizontal turbulence intensity profiles for the IRT vent tower area.

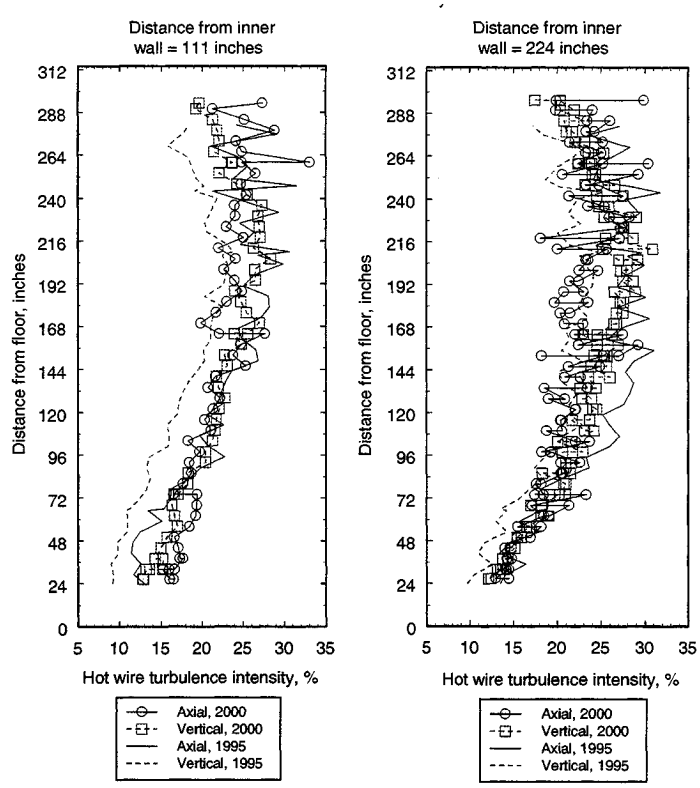

Figure 13.—Vertical turbulence intensity profiles for the IRT vent tower area.

(c)2001 American Institute of Aeronautics & Astronautics or Published with Permission of Author(s) and/or Author(s)' Sponsoring Organization.

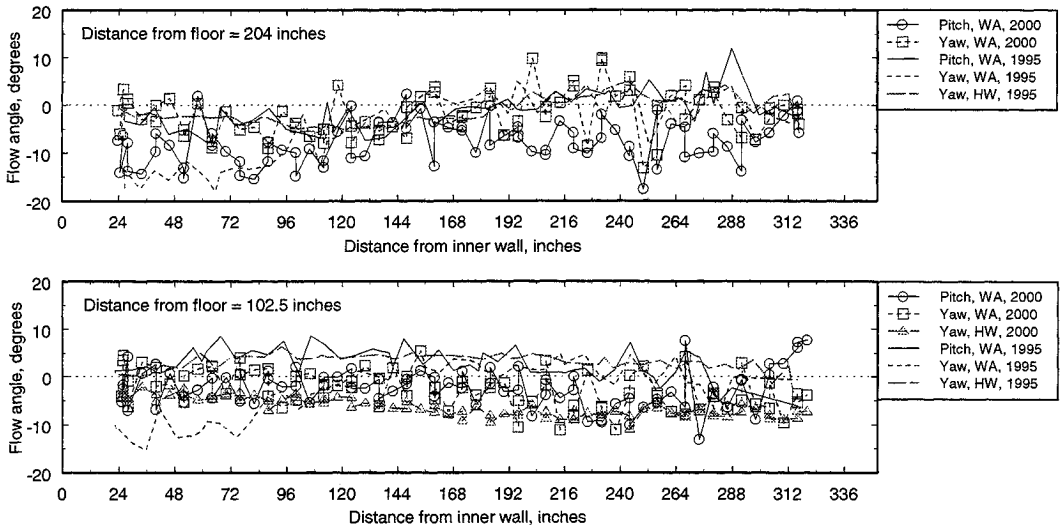

Figure 14.—Horizontal pitch and yaw flow angle profiles for the IRT vent tower area.

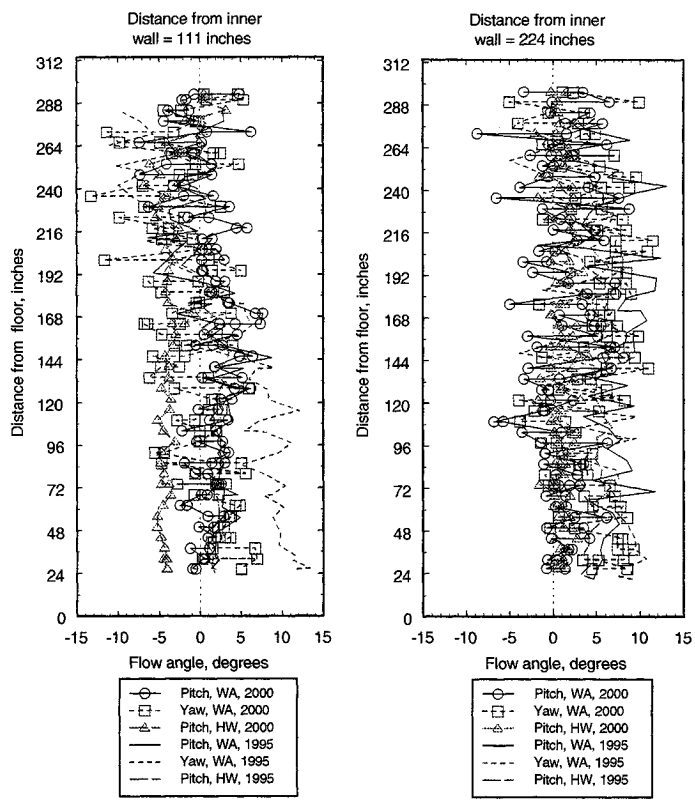

Figure 15.—Vertical pitch and yaw flow angle profiles for the IRT vent tower area.

(c)2001 American Institute of Aeronautics & Astronautics or Published with Permission of Author(s) and/or Author(s)' Sponsoring Organization.

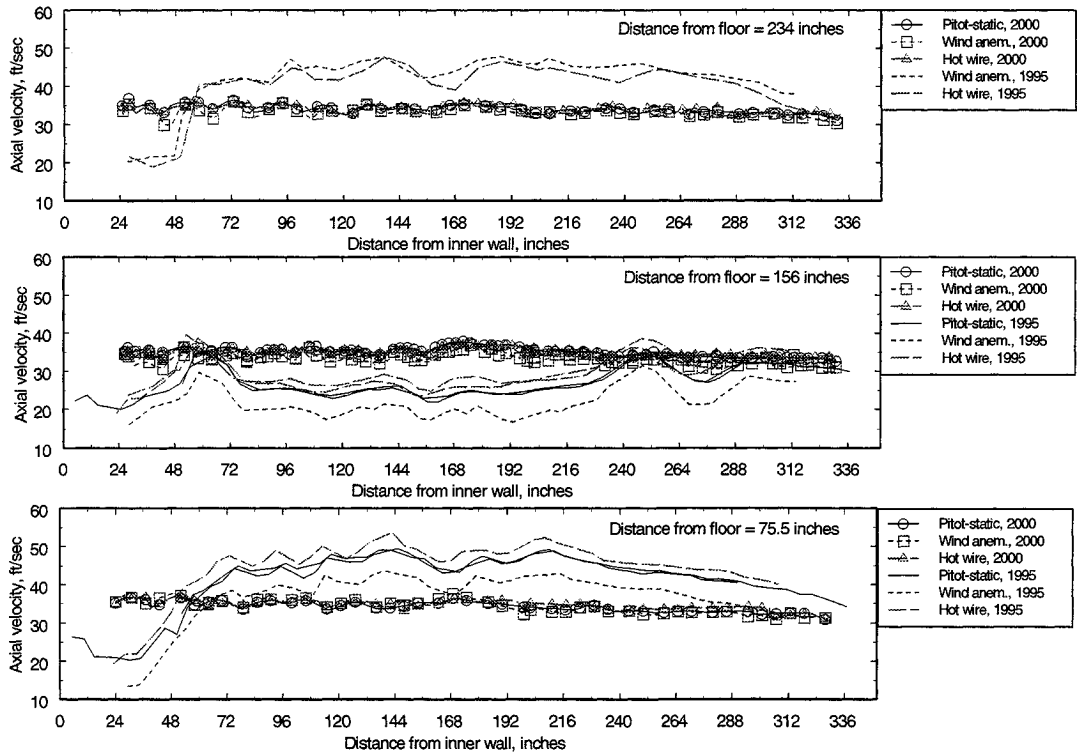

Figure 16.—Horizontal velocity profiles for the IRT settling chamber.

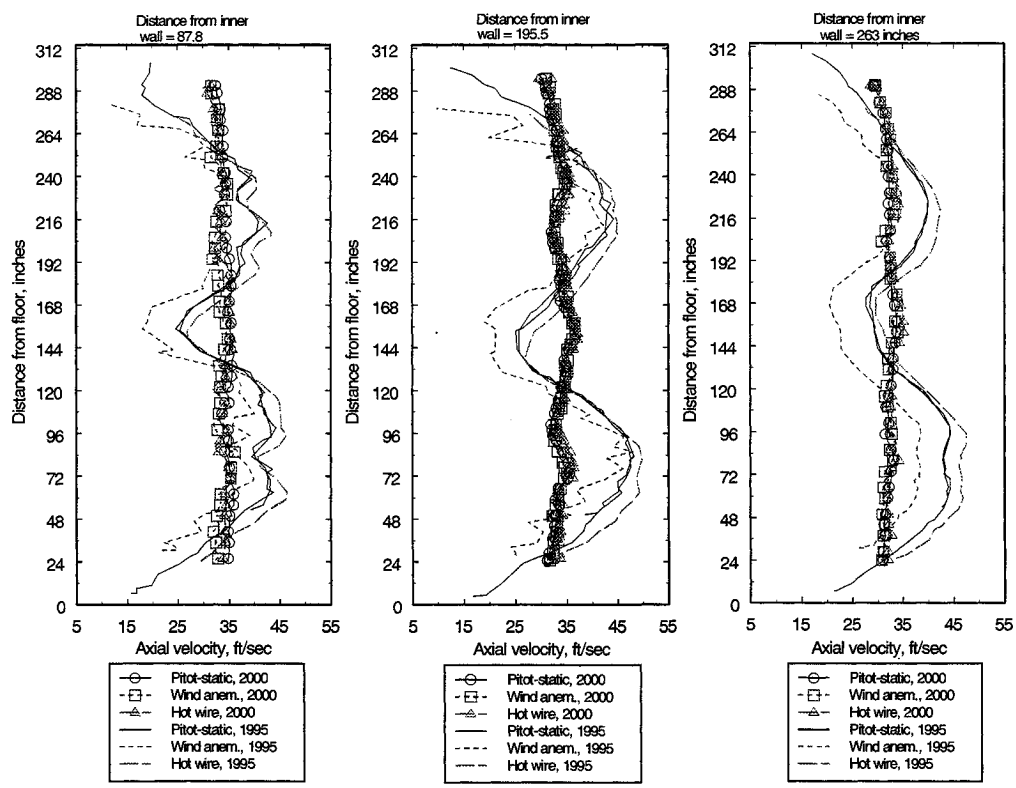

Figure 17.—Vertical velocity profiles for the IRT settling chamber.

(c)2001 American Institute of Aeronautics & Astronautics or Published with Permission of Author(s) and/or Author(s)' Sponsoring Organization.

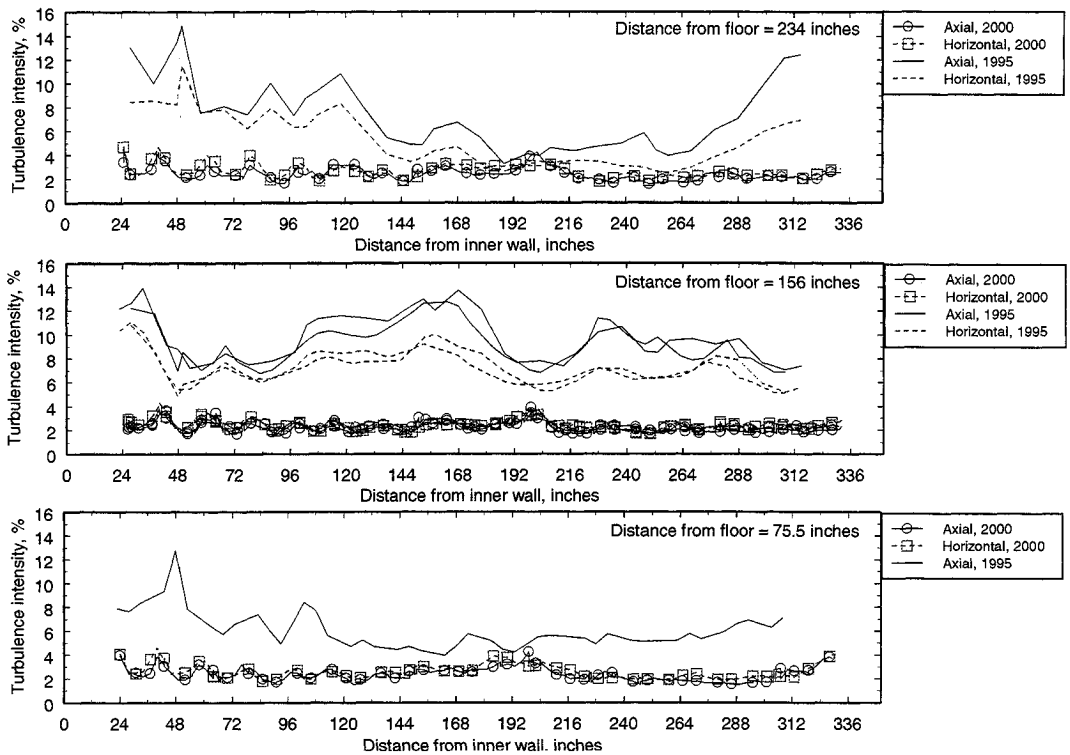

Figure 18.—Horizontal turbulence intensity profiles for the IRT settling chamber.

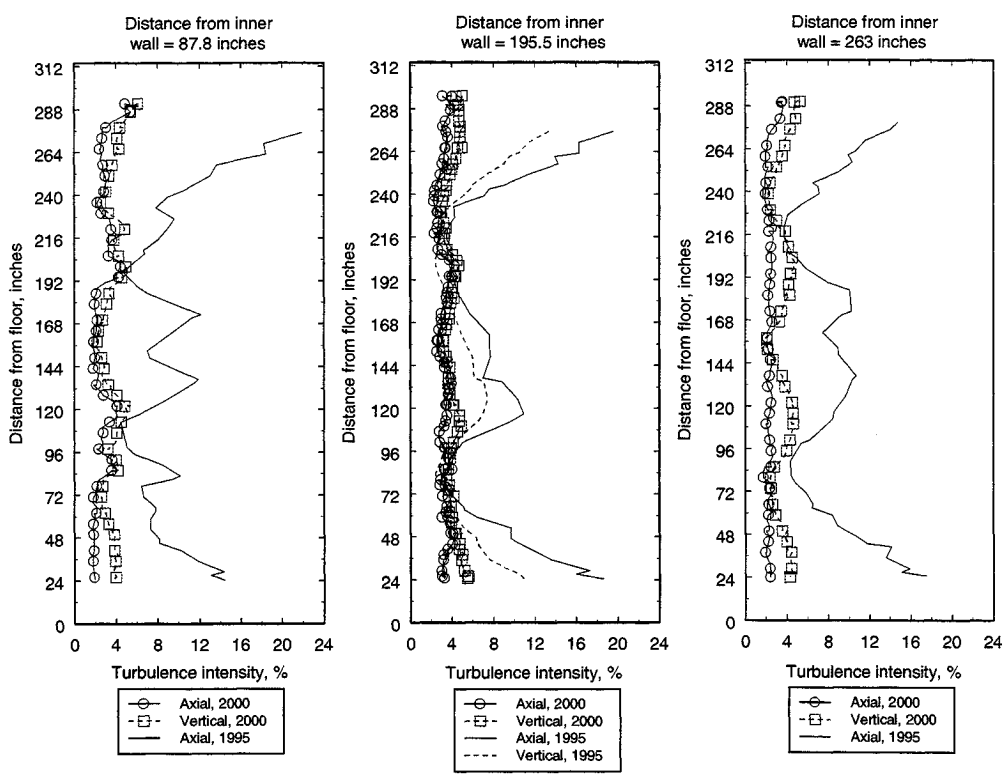

Figure 19.—Vertical turbulence intensity profiles for the IRT settling chamber.

(c)2001 American Institute of Aeronautics & Astronautics or Published with Permission of Author(s) and/or Author(s)' Sponsoring Organization.

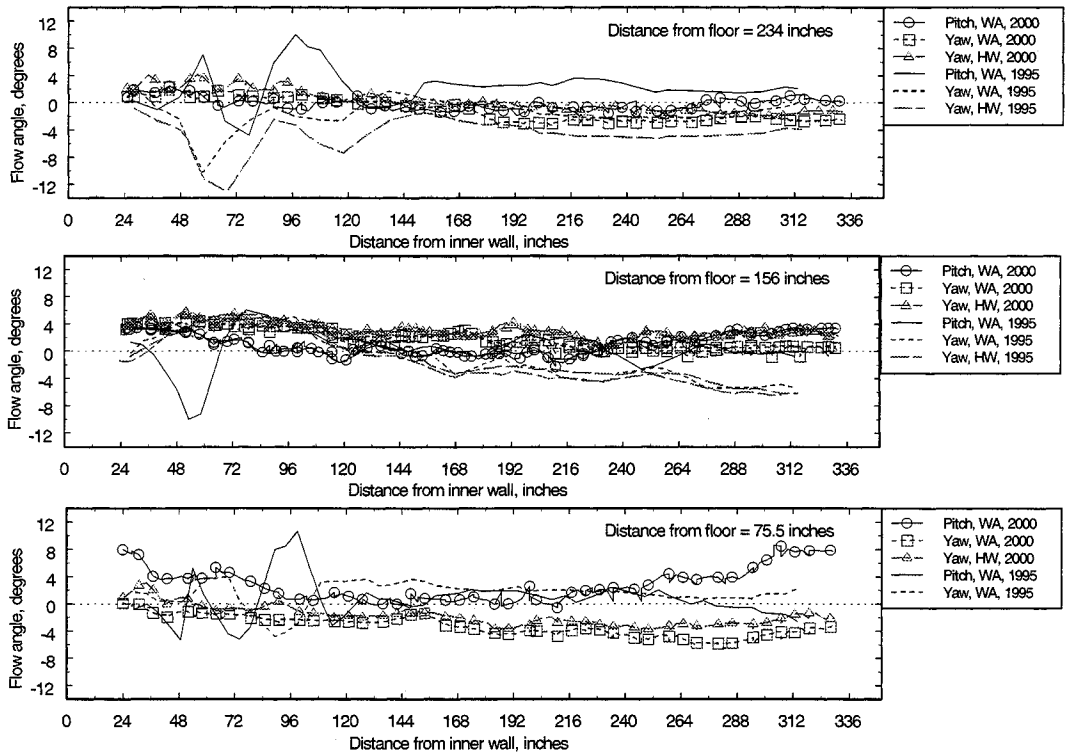

Figure 20.—Horizontal pitch and yaw flow angle profiles for the IRT settling chamber.

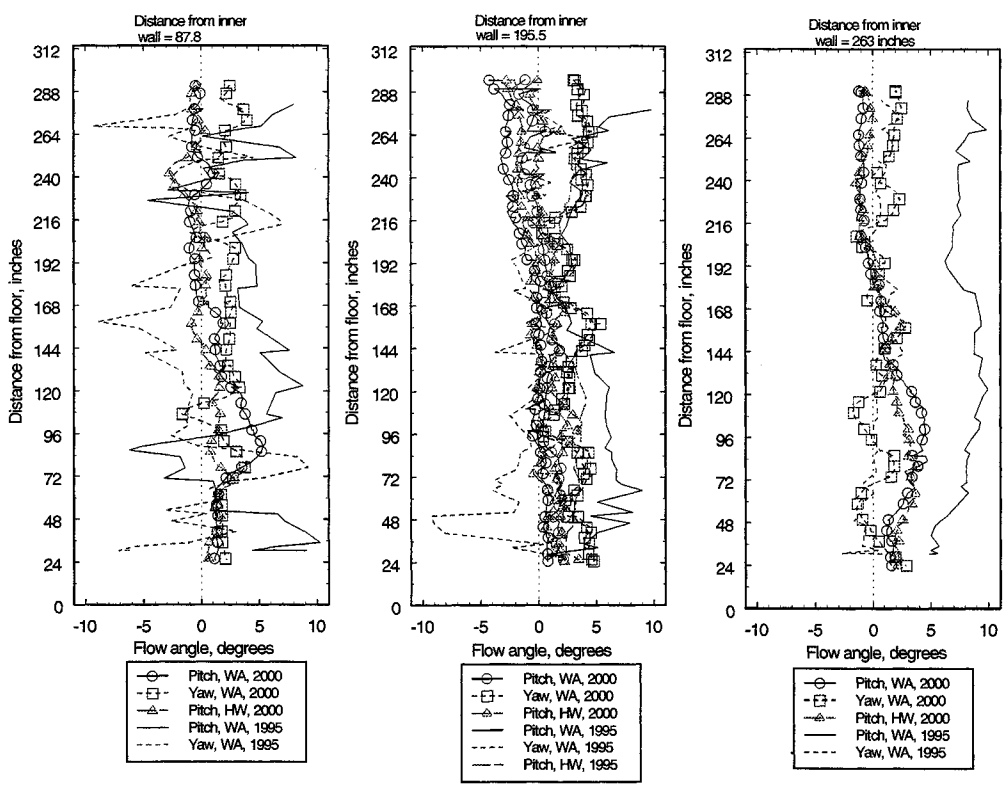

Figure 21.—Vertical pitch and yaw flow angle profiles for the IRT settling chamber.